RNA editing of *SLC22A3* drives early tumor invasion and metastasis in familial esophageal cancer

Li Fu[a,b,1,2], Yan-Ru Qin[c,1], Xiao-Yan Ming[d,1], Xian-Bo Zuo[e,f,1], Yu-Wen Diao[a,b,1], Li-Yi Zhang[d], Jiaoyu Ai[c], Bei-Lei Liu[a,b], Tu-Xiong Huang[a,b], Ting-Ting Cao[a,b], Bin-Bin Tan[a,b], Di Xiang[a,b], Chui-Mian Zeng[a,b], Jing Gong[g,h,i], Qiangfeng Zhang[g,h,i], Sui-Sui Dong[d], Juan Chen[d], Haibo Liu[j], Jian-Lin Wu[k], Robert Z. Qi[l], Dan Xie[m], Li-Dong Wang[n], and Xin-Yuan Guan[d,m,2]

[a]Department of Pharmacology, Shenzhen University School of Medicine, Shenzhen, China 518060; [b]Cancer Research Centre, Health Science Center, Shenzhen University, Shenzhen, China 518060; [c]Department of Clinical Oncology, the First Affiliated Hospital, Zhengzhou University, Zhengzhou, China 450000; [d]Department of Clinical Oncology, University of Hong Kong, Hong Kong, China; [e]Department of Dermatology, the First Affiliated Hospital of Anhui Medical University, Hefei, China 230000; [f]State Key Laboratory Incubation Base of Dermatology, Ministry of National Science and Technology, Hefei, China 230000; [g]MOE Key Laboratory of Bioinformatics, Tsinghua University, Beijing 100084, China; [h]Center for Synthetic and Systems Biology, Tsinghua University, Beijing 100084, China; [i]Center for Tsinghua-Peking Joint Center for Life Sciences, School of Life Sciences, Tsinghua University, Beijing 100084, China; [j]Key Laboratory for Major Obstetric Diseases of Guangdong Province, The Third Affiliated Hospital of Guangzhou Medical University, Guangzhou, China 510150; [k]State Key Laboratory for Quality Research in Chinese Medicines, Macau University of Science and Technology, Macau, China; [l]Department of Biochemistry, Hong Kong University of Sciences and Technology, Hong Kong, China; [m]State Key Laboratory of Oncology in Southern China, Cancer Center, Sun Yat-Sen University, Guangzhou, China 510275; and [n]Henan Key Laboratory for Esophageal Cancer Research of the First Affiliated Hospital, Zhengzhou University, Zhengzhou, Henan, China 450000

Like many complex human diseases, esophageal squamous cell carcinoma (ESCC) is known to cluster in families. Familial ESCC cases often show early onset and worse prognosis than the sporadic cases. However, the molecular genetic basis underlying the development of familial ESCC is mostly unknown. We reported that *SLC22A3* is significantly down-regulated in nontumor esophageal tissues from patients with familial ESCC compared with tissues from patients with sporadic ESCCs. A-to-I RNA editing of the *SLC22A3* gene results in its reduced expression in the nontumor esophageal tissues of familial ESCCs and is significantly correlated with lymph node metastasis. The RNA-editing enzyme *ADAR2*, a familial ESCC susceptibility gene identified by our post hoc genome-wide association study, is positively correlated with the editing level of *SLC22A3*. Moreover, functional studies showed that *SLC22A3* is a metastasis suppressor in ESCC, and deregulation of *SLC22A3* facilitates cell invasion and filopodia formation by reducing its direct association with α-actinin-4 (ACTN4), leading to the increased actin-binding activity of ACTN4 in normal esophageal cells. Collectively, we now show that A-to-I RNA editing of *SLC22A3* contributes to the early development and progression of familial esophageal cancer in high-risk individuals.

RNA editing | metastasis suppressor | familial ESCC | SLC22A3 | ADAR2

Esophageal carcinoma (EC) is ranked as the sixth leading cause of death from cancer worldwide (1). Esophageal squamous cell carcinoma (ESCC) is the major histological subtype of EC and is characterized by its remarkable geographic distribution internationally and within China (2–6). ESCC occurs with the highest frequency among the Chinese, especially the high-risk Northern Chinese, where the incidence rate is 121 per 100,000 people, more than 20 times higher than in low-risk regions worldwide (7). Within these high-risk regions, studies have shown a strong tendency toward familial aggregation, suggesting that host genetic susceptibility, in conjunction with potential environmental exposures, may be involved in the etiology of this cancer (8, 9).

The conventional approach for the identification of familial susceptibility gene is to identify its chromosomal localization by linkage analysis and subsequently to isolate the target susceptibility gene by positional cloning. A successful linkage analysis depends on the collection of satisfactory familial samples. However, it is almost impossible to collect satisfactory familial samples, because most of ESCC-affected members in the family had died when a proband was found. Therefore, alternative strategies should be used to identify the susceptibility gene in familial ESCC. Several studies have concentrated on elucidating

the high frequency of familial ESCC in Shanxi, China (10–14). These earlier studies using genome-wide allelotyping of familial ESCC cases showed that 13q and 17p loss was significantly associated with ESCC development (10–12). Gene chip and SNP arrays were also used for studying the molecular mechanisms underlying familial ESCC (13, 14). Moreover, previous clinical study suggested that familial esophageal cancer may develop earlier and have a poorer prognosis than sporadic esophageal cancer (15). However, the molecular genetic basis underlying the early development and progression of familial ESCC is mostly unknown.

To identify potential genes that contribute to the development and progression of familial ESCC, we compared gene-expression profiles of tumor and adjacent nontumor (NT) tissues from five familial ESCC specimens using the Affymetrix human genome U133 Plus 2.0 GeneChip. The present study identified a number of

Significance

Familial esophageal squamous cell carcinoma (ESCC) often shows early onset and worse prognosis. Little is known about the genetic basis underlying the pathogenesis of familial ESCC. To identify the genetic alterations associated with familial ESCC susceptibility, we compared the gene-expression profiles of familial and sporadic ESCCs. We found that A-to-I RNA editing–mediated downregulation of *SLC22A3* is almost exclusively present in familial ESCC and may serve as a potential biomarker for familial ESCC patients. Molecular mechanism study further revealed that a single mutation at the RNA level could change the protein structure of SLC22A3, leading to a loss of inhibitory capability for the metastasis-promoting protein ACTN4. Our findings provide insights that may lead to more effective clinical management of individuals at high risk of familial ESCC with *SLC22A3* deregulation.

differentially expressed genes that were related to cell development, cell motility, and immunity in familial ESCC, compared with both NT and previously reported sporadic ESCC (16). One gene, *SLC22A3* (or organic cation transporter 3, *OCT3*), caught our attention because it was previously reported to be one of the important risk loci for prostate (17) and colon cancer (18, 19). The *SLC22A3* gene encodes a cation transport protein belonging to the SLC22A family (SLC22A1-3 or OCT1-3), which is critical for drug transportation and cellular detoxification (20, 21). Moreover, it has been reported that aberrant methylation contributes to the reduced expression of *SLC22A3* in prostate cancer (22), indicating a tumor-suppressive role for *SLC22A3* in human cancers.

In the present work, we addressed the role of *SLC22A3* in the molecular pathogenesis of familial ESCC. We reported that *SLC22A3* is significantly down-regulated in NT esophageal tissues from familial ESCC patients compared with those from sporadic ESCCs. A-to-I RNA editing of the *SLC22A3* gene is found to be significantly associated with the reduced *SLC22A3* transcription and lymph node metastasis in the familial ESCCs. The editing level of *SLC22A3* is regulated by the RNA-editing enzyme *ADAR2*. We also used molecular genetic studies to characterize the *SLC22A3* gene and investigated the mechanism of alteration.

Results

Identification of Differentially Expressed Genes in Familial ESCC.
Gene-expression profiles of five familial ESCCs and their normal counterparts were obtained by microarray analysis. The five familial ESCC cases were from an ESCC high-risk area (Henan province), and were selected when the family had at least four ESCC cases within three generations or at least five patients in two generations (Fig. S1A). To identify further the genes differentially expressed in familial and sporadic ESCC, we compared the expression profiles of familial tumors with both NT

tissue and previously reported sporadic tumors (16). Using an arbitrary cutoff of signal log ratio ≥2.0, we found that 180 genes with known function were significantly deregulated in familial tumor (113 up-regulated and 67 down-regulated) compared with both NT and sporadic tumors (Fig. S1 *B and C* and Tables S1 and S2). To study associated biological annotation, Database for Annotation, Visualization and Integrated Discovery (DAVID) gene ontology (GO) analysis was performed on the 180 differentially expressed genes (23). A selection of significant GO terms is shown for biological processes, molecular functions, and cellular component of 113 up-regulated (Fig. S1D) and 67 down-regulated genes (Fig. S1E).

Frequent Down-Regulation of *SLC22A3* in Familial ESCC.
As one of many potentially relevant genes on the down-regulated gene list, *SLC22A3* drew our attention because it appears in two of the top three enriched GO biological processes: response to organic substance and response to extracellular stimulus (Fig. S1E). Several lines of evidence demonstrated in the Introduction also suggested that *SLC22A3* might be an epigenetically regulated cancer-related gene. We therefore selected this gene for further study in familial ESCC. Initially, quantitative PCR (qPCR) was performed to validate *SLC22A3* expression levels in familial (n = 50) and sporadic (n = 100) ESCC cohorts. As shown in Fig. 1A, the mean level of *SLC22A3* expression was reduced significantly in familial tumors compared with the corresponding NT tissues [change in cycle threshold (ΔCt) value 14.65 ± 0.64 vs. 11.26 ± 0.39, respectively; P < 0.0001) (higher ΔCt values correspond to lower expression). However, no significant difference in the mean level of *SLC22A3* expression was observed between ESCC tumors and their counterparts in the sporadic cohorts (9.17 ± 0.32 vs. 8.67 ± 0.23, respectively; P = 0.517). Notably, of the two ESCC cohorts, the mean expression level of *SLC22A3* was significantly lower in familial than in sporadic NT tissues (P < 0.0001)
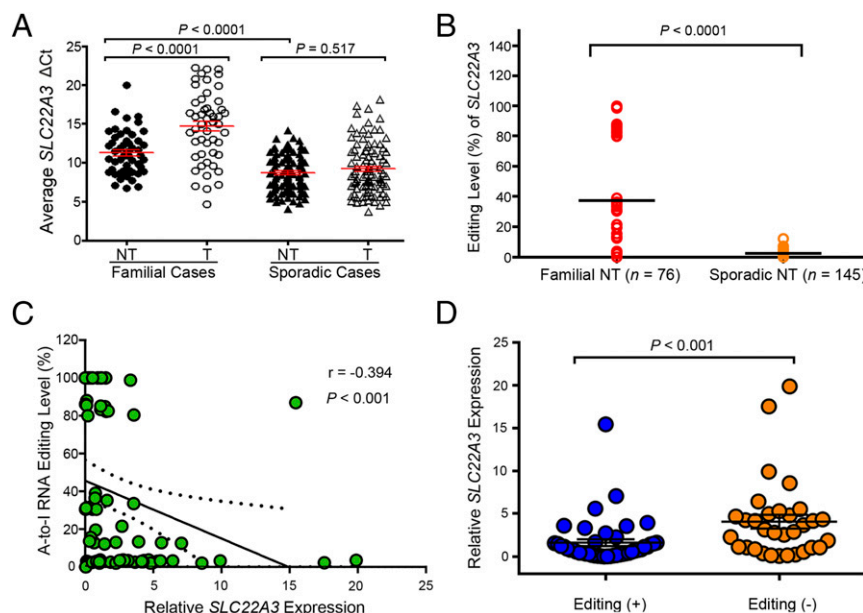
Fig. 1. A-to-I RNA editing contributes to the down-regulation of *SLC22A3* in familial ESCC. (*A*) qPCR was used to detect *SLC22A3* transcripts in the familial (n = 50) and sporadic (n = 100) cohorts. Each cohort contains primary ESCC tumors (T) and matched adjacent NT tissues. Dot plots represent the ΔCt values of *SLC22A3* (higher ΔCt values correspond to lower expression; mean ± SEM; Mann–Whitney *U* test. (*B*) Dot plots represent the *SLC22A3* editing levels, determined by pyrosequencing, detected in the NT cDNA samples from patients with familial (n = 76) and sporadic (n = 145) ESCC. Horizontal black lines indicate the mean value. P < 0.0001 by the Mann–Whitney *U* test. (*C*) Negative correlation between the relative expression level of *SLC22A3* and A-to-I RNA editing level in NT specimens from 76 patients with familial ESCC, expressed using Spearman's correlation coefficients. The linear regression is shown as a solid line, and 95% CIs are shown by dotted lines. (*D*) Dot plots represent the relative expression of *SLC22A3* in familial NT cDNA samples stratified by editing status, with (Editing +) and without (Editing −) A-to-I RNA editing. Data are presented as the mean ± SEM; P < 0.001 by the Mann–Whitney *U* test.

(Fig. 1*A*). These observations not only confirmed our previous array data but also suggest the involvement of *SLC22A3* in the early development of ESCC in individuals at high risk of familial ESCC.

Frequent A-to-I *SLC22A3* RNA Editing in Familial ESCC. To look for a possible gene-regulation mechanism of *SLC22A3*, we initially determined its coding region in 20 pairs of cDNA samples from familial ESCC tumors and their adjacent NT tissues by Sanger sequencing. Although we found no evidence of mutations in the *SLC22A3* coding region, an A-to-I transcript-editing event (A261 at exon 1), leading to an asparagine (Asn)-to-aspartic acid (Asp) amino acid substitution, was identified in the cDNA but not in the matched genomic DNA samples (Fig. S2*A*). To quantify the editing level of *SLC22A3*, pyrosequencing was applied, and the results were consistent with the Sanger sequencing data from the 20 familial ESCCs (Fig. S2*B*). We thus extended the pyrosequencing study to examine the *SLC22A3* editing level in normal esophageal epithelia from 76 familial and 145 sporadic ESCCs. *SLC22A3*-positive editing (defined as the percentage of G signal ≥5%) was detected in 44/76 (57.9%) familial and 3/145 (2.1%) sporadic NT samples. The mean editing level of *SLC22A3* was significantly higher in familial than in sporadic NT samples (37.6 vs. 2.3, respectively; $P < 0.0001$) (Fig. 1*B*). *SLC22A3* editing was not detected in peripheral blood mononuclear cells and other normal human tissues (Fig. S3). These findings indicated that A-to-I *SLC22A3* RNA editing is prominently associated with familial ESCC and predisposes these high-risk individuals to develop esophageal cancer.

***SLC22A3* RNA Editing Contributes to Its Down-Regulation in Familial ESCC.** To determine whether down-regulation of *SLC22A3* is regulated by the RNA editing, the correlation between *SLC22A3* editing and transcription level was analyzed. *SLC22A3* RNA editing showed a significantly negative correlation with its mRNA level in the 76 familial NT tissues (Spearman's $r = −0.394$, $P < 0.001$) (Fig. 1*C*). Moreover, we compared the mean *SLC22A3* expression levels in familial NT samples with and without editing. The results showed that *SLC22A3* transcript was significantly reduced in the positive-editing group compared with the no editing-group, indicating that form of A-to-I *SLC22A3* RNA may have decreased stability in familial cases ($P < 0.001$) (Fig. 1*D*).

Deregulated *SLC22A3* Is an Early Risk Factor for Progression of Familial ESCC. Furthermore, we investigated the clinical associations with *SLC22A3* editing status obtained from NT samples in this familial ESCC cohort. As shown in Fig. 2*A*, edited *SLC22A3* was significantly correlated with lymph node metastasis ($P = 0.002$) but not with other clinicopathological factors (e.g., age, sex, T stage, differentiation). Because vascular endothelial growth factor C (*VEGFC*) is a factor known to cause lymphangiogenesis (24), we examined the mRNA level of *VEGFC* in the same familial cohort. The results showed a reverse correlation between *SLC22A3* and *VEGFC* expression in familial NT tissues (Spearman's $r = −0.306$, $P = 0.007$) (Fig. 2*B*), indicating that deregulated *SLC22A3* is an early event leading to the malignant development and progression of familial ESCCs.

RNA-Editing Enzyme *ADAR2* Contributes to *SLC22A3* Editing in Familial ESCC. A-to-I RNA editing is known to be catalyzed by members of the RNA-editing enzyme ADAR (adenosine deaminase acting on RNA) family (25). Interestingly, we found that one of the human ADAR members, *ADAR2* (also known as "*ADARB1*"), is located at 21q22.3, a newly identified ESCC susceptibility locus by genome-wide association study (GWAS) (26). We thus performed a post hoc GWAS analysis to investigate the influence of common genetic variants around the *ADAR2* gene region on ESCC risk. We selected 291 genetic variants around the *ADAR2* gene region from the dataset of a previously reported GWAS in 496 ESCC cases with

a family history of upper gastrointestinal tract cancers and 1,056 healthy controls (27). The results showed that one SNP (rs3788157) within intron 1 of *ADAR2* is significantly associated with ESCC risk in the familial cases, suggesting that *ADAR2* could be a susceptibility gene for familial ESCC ($P = 2.90E-02$, odds ratio = 1.247, 95% CI 1.239–1.255) (Fig. 2*C*). To investigate whether *ADAR2* could regulate *SLC22A3* editing, we first examined the *ADAR2* expression levels in the NT tissues from familial ($n = 76$) and sporadic ($n = 145$) ESCC cohorts. As shown in Fig. 2*D*, the average ΔCt value was significantly lower in the familial NT samples than in the sporadic samples (7.59 vs. 10.05, $P < 0.0001$), suggesting that the *ADAR2* transcripts were specifically increased in the familial NT samples. Moreover, the correlation analyses demonstrated that the *ADAR2* expression level was positively correlated with the *SLC22A3* editing level (Spearman's $r = 0.699$, $P < 0.0001$) (Fig. 2*E*), suggesting that *ADAR2* is responsible for the regulation of *SLC22A3* editing in familial ESCC.

***SLC22A3* Is a Metastasis Suppressor in ESCC.** To explore the functional consequences of depleted or edited *SLC22A3* in ESCC, we initially examined *SLC22A3* expression in 10 esophageal cell lines. Both qPCR and immunoblotting showed that *SLC22A3* expression was significantly down-regulated in seven of nine (77.8%) ESCC cell lines compared with the immortalized normal esophageal epithelial cell line NE1 (Fig. S4). We then established KYSE30 and KYSE180 cells lacking endogenous *SLC22A3* expression with stable overexpression of wild-type/edited (A261 > G) *SLC22A3* (KYSE30/KYSE180-*wt*/SLC22A3 or -*edit*/SLC22A3) by lentiviral transduction. Empty-vector–transfected (KYSE30-EV) cells were used as controls. The transduction efficiency was confirmed using qPCR and Western blotting (Fig. 3*A*). Ectopic *SLC22A3* expression in KYSE30/KYSE180 cells (KYSE30/KYSE180-*wt*/SLC22A3 or -*edit*/SLC22A3) had no effect on cell growth (Fig. S5*A*) or on the efficiency of foci formation (Fig. S5*B*) compared with control cells. However, cell-adhesion assays demonstrated that wild-type *SLC22A3* had increased but edited *SLC22A3* had decreased cell-adhesion ability compared with control cells (Fig. 3*B*). Additionally, both wound-healing and invasion assays showed that wild-type *SLC22A3* had inhibitory effects on ESCC cell migration and invasion, whereas edited *SLC22A3* displayed loss of inhibitory function compared with control cells (Fig. 3 *C* and *D*). To analyze whether the loss-of-function phenotypes are regulated in an edited *SLC22A3*–dependent manner, we mixed the KYSE30-*wt*/SLC22A3 cells in five different percentages (0, 10, 20, 40, and 80%, respectively) of KYSE30-*edit*/SLC22A3 cells (30-wt, 30-edit1, 30-edit2, 30-edit3, and 30-edit4, respectively). Compared with 30-wt cells, cell migration and invasion abilities were progressively increased from 30-edit2 cells harboring 20% edited *SLC22A3* transcripts to 30-edit4 cells harboring 80% edited *SLC22A3* transcripts, demonstrating that tumorigenic properties correlate with *SLC22A3* editing level (Fig. S6 *A* and *B*). To determine further whether wild-type *SLC22A3* inhibits cell migration/invasion by suppressing the epithelial–mesenchymal transition (EMT), the expressions of epithelial marker (E-cadherin), mesenchymal markers (Vimentin and α-SMA), and EMT regulators (Snail and MMP9) were examined in KYSE30-*wt*/SLC22A3, KYSE30-*edit*/SLC22A3, and control cells by Western blotting. The results showed that E-cadherin was significantly up-regulated, whereas Vimentin, α-SMA, Snail, and MMP9 were down-regulated in KYSE30-*wt*/SLC22A3 cells compared with KYSE30-*edit*/SLC22A3 and control cells, suggesting that wild-type *SLC22A3* could inhibit ESCC cell migration/invasion via a reversal of EMT process (Fig. S7). Furthermore, using a lymph node metastatic mouse model, we found strong metastasis-suppressing ability in wild-type KYSE30 cells overexpressing *SLC22A3* but not in the edited clones overexpressing *SLC22A3*
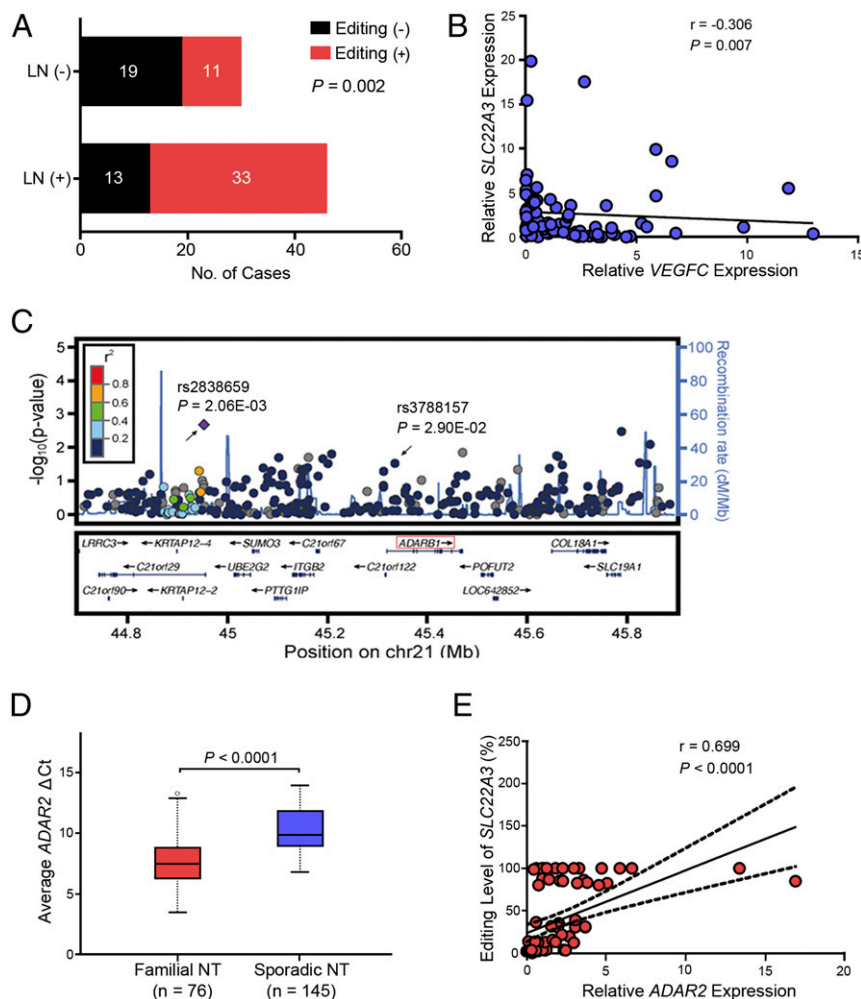
Fig. 2. *ADAR2*-mediated RNA editing of *SLC22A3* in familial ESCC. (*A*) The bar chart represents the correlation between the editing status of *SLC22A3* and lymph node (LN) metastasis in 76 cases of familial ESCC ($P = 0.002$, χ^2 test). (*B*) Negative correlation between the relative expression level of *SLC22A3* and the lymphangiogenesis inducer *VEGFC* in NT specimens from 76 cases of familial ESCC, expressed using Spearman's correlation coefficients. The solid line indicates the linear regression. (*C*) Regional association plots for the *ADAR2* gene at 21q22.3. Shown are the *P* values ($-\log_{10}$ scale) of the association tests for genotyped (diamond) and imputed (circles) SNPs in the discovery sample. Genetic recombination rates are represented by light-blue lines, and genes within the regions are indicated by arrows. (*D*) Tukey boxplots represent the ΔCt values of *ADAR2* detected by qPCR in the NT specimens from familial ($n = 76$) and sporadic ($n = 145$) ESCCs. The horizontal black line indicates the median value; open circles indicate outliers; $P < 0.0001$ by the Mann–Whitney *U* test. (*E*) Positive correlation between the relative expression of *ADAR2* and *SLC22A3* editing levels in NT specimens from 76 patients with familial ESCC, expressed using Spearman's correlation coefficients The solid line shows the linear regression; dotted lines indicate the 95% CI.

compared with control cells (P = 0.02) (Fig. 3*E*). These results demonstrated that *SLC22A3* has a strong metastasis-suppressive ability in ESCC.

Depletion of *SLC22A3* Promotes Normal Esophageal Cell Motility. Moreover, we established NE1 cells showing wild-type *SLC22A3* with *SLC22A3* stable knockdown (NE1-shSLC22A3-1/-2) by lentiviral transduction (Fig. 4 *A–C*). Nontemplate shRNA-transfected (NE1-NTC) cells were used as controls. ShRNA-mediated depletion of wild-type *SLC22A3* in NE1 had no effect on cell growth (Fig. 4*D*) compared with control cells. However, both wound-healing and invasion assays showed that *SLC22A3* knockdown had strong promoting effects on NE1 cell migration and invasion compared with control cells (Fig. 4 *E* and *F*), further supporting the notion that deregulated *SLC22A3* may contribute to the early development and progression of ESCC.

SLC22A3 Interacts with ACTN4 and Inhibits ACTN4-Induced Cell Invasion. To look for the molecular mechanisms underlying the opposite effects on cell migration, invasion, and metastasis conferred

by wild-type and edited *SLC22A3*, we initially performed coimmunoprecipitation (co-IP) and mass spectrometry using Flag-tagged wild-type or edited *SLC22A3*-transfected KYSE30 cells (Fig. 5*A*) and identified 27 proteins potentially interacting with wild-type SLC22A3 but not with the edited form (Table S3). Notably, ACTN4 is the highest-ranked SLC22A3-interacting protein involved in cell motility (Fig. 5*A*) (28). To confirm the interactions between SLC22A3 and ACTN4 in wild-type or edited KYSE30 cells overexpressing *SLC22A3*, the whole-cell lysates from these two clones were subjected first to immunoprecipitation (IP) with anti-Flag antibody bound to protein G-Sepharose beads. Then, the immunoprecipitates were subjected to Western blotting analysis using anti-SLC22A3 and anti-ACTN4 antibodies. The amount of endogenous ACTN4 precipitated by anti-Flag antibody was remarkably reduced in edited clones overexpressing *SLC22A3* compared with wild-type clones overexpressing *SLC22A3* (Fig. 5*B*). The specific interaction between SLC22A3 and ACTN4 was also detected by reverse co-IP experiments. When the cell lysates were subjected to IP with anti-ACTN4 antibody, wild-type
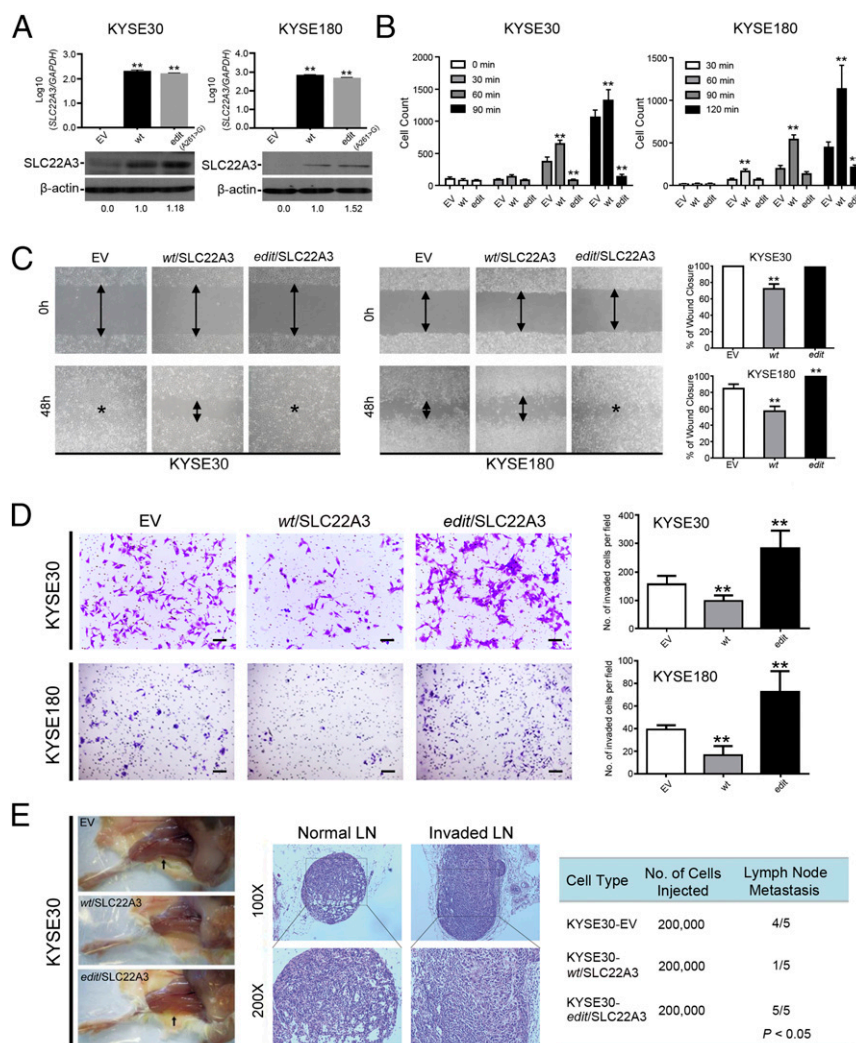
Fig. 3. *SLC22A3* has a strong metastasis-suppressive role. (*A*) Overexpression of wild-type and edited *SLC22A3* in KYSE30 (KYSE30-*wt*/SLC22A3 and KYSE30-*edit*/SLC22A3) or KYSE180 (KYSE180-*wt*/SLC22A3 and KYSE180-*edit*/SLC22A3) clones was confirmed by qPCR (*Upper*) and Western blotting (*Lower*). Empty-vector–transfected (KYSE30/KYSE180-EV) cells were used as controls. (*B*) An adhesion assay was used to detect cell-adhesion ability in wild-type or edited KYSE30 and KYSE180 cells overexpressing *SLC22A3* in the indicated time periods. Empty-vector–transfected cells were used as control. The cell numbers were counted from three independent experiments. **$P < 0.001$, ANOVA with post hoc test. (*C*) The effect of *SLC22A3* on cell migration was determined using the wound-healing assay. Representative images show that wild-type *SLC22A3*-transfected cells migrated more slowly along the wound edge than the edited *SLC22A3*-transfected cells and control cells. The percentage of wound closure is shown as mean $\pm$ SD of three independent experiments; **$P < 0.01$, ANOVA with post hoc test. (*D*) Representative images (*Left*) and quantification of cells (*Right*) from the indicated KYSE30 and KYSE180 clones that invaded through Matrigel-coated membrane. Results are shown as the mean $\pm$ SD of three independent experiments. (Scale bar: 200 μm.) **$P < 0.01$, ANOVA with post hoc test. (*E*, *Left*) Representative images of popliteal lymph nodes (LNs) in SCID mice following s.c. footpad injection of the indicated KYSE30 clones. Black arrows point to the popliteal LN. (*Center*) Representative H&E staining of normal LNs and tumor cell-invaded LNs from tested animals (original magnification: 100×). (*Right*) The numbers of metastatic popliteal LNs in each group of animals were summarized ($P < 0.05$, χ^2 test).

SLC22A3 was specifically precipitated with ACTN4, but the edited form of SLC22A3 showed less binding to ACTN4 (Fig. 5C). ACTN4 is an actin-binding protein that cross-links actin filaments into bundles to form filopodia (29). The amount of actin in the IP fraction precipitated by anti-ACTN4 antibody was also significantly reduced in wild-type clones overexpressing *SLC22A3* as compared with edited clones overexpressing *SLC22A3*, suggesting that ACTN4-mediated actin crosslinking was inhibited by wild-type SLC22A3 (Fig. 5C). Moreover, double-immunolabeling was performed with anti-Flag/anti–F-actin and anti-ACTN4 antibodies. Wild-type SLC22A3 and ACTN4 were colocalized primarily at the cell membrane, whereas edited SLC22A3 was presented mainly in the cytoplasm and showed significantly reduced colocalization with ACTN4 ($P < 0.001$) (Fig. 5 D and E). In contrast, colocalization between F-actin and ACTN4 was significantly

increased in edited clones overexpressing *SLC22A3* as compared with wild-type clones overexpressing *SLC22A3* ($P = 0.019$) (Fig. 5 D and E). Furthermore, we predicted the protein conformation of SLC22A3 by building a homology model with the Rebetta tool from David Baker's group [robetta.bakerlab.org/]. As shown in Fig. 5F, wild-type SLC22A3 is a transmembrane protein (cyan). We also build the structure model for the mutation form (by A-to-I editing) of SLC22A3-N72D (purple) (Fig. 5G). The main part of the protein does not change except for the N-terminal and the coils in the extracellular region (30). Although the N-terminal difference may be caused by thermodynamic fluctuations, the changes in the extracellular region are likely caused by the mutation of residue N72, which is at the center of the structure changes (yellow spheres in Fig. 5F). As we know, ACTN4 is a key element of filopodia, which form focal adhesions with the substratum at the cell surface. We did predict a

Fig. 4. *SLC22A3* knockdown increases normal esophageal cell motility. (*A*) The percentage of edited *SLC22A3* transcripts was determined by pyrosequencing in normal esophageal NE1cells. (*B* and *C*) Expression of *SLC22A3* in shSLC22A3 stably transfected NE1 clones (NE1-shSLC22A3-1 and -2) was confirmed by qPCR (*B*) and Western blotting (*C*). Nontemplate shRNA-transfected cells (NE1-NTC) were used as controls. **$P < 0.001$, ANOVA with post hoc test. (*D*) Relative growth rates of *SLC22A3*-repressed NE1 cells were compared with control cells by XTT assay. The results are expressed as the mean $\pm$ SD of at least three independent experiments. $P > 0.05$; ANOVA. (*E*) The effect of depleted *SLC22A3* on cell migration was determined using the wound-healing assay. Representative images show that *SLC22A3*-repressed NE1 cells migrated faster along the wound edge than the control cells. (*F*) The representative images (*Left* and *Upper Right*) and quantification of cells (*Lower Right*) from the indicated NE1 cells that invaded through Matrigel-coated membrane. Results are shown as mean $\pm$ SD of three independent experiments. (Scale bars: 200 μm.) **$P < 0.001$, ANOVA with post hoc test.

potential binding interface for wild-type SLC22A3 in the extracellular region (red sticks in Fig. 5*F*) (31). As can be seen from the comparison of the two models (Fig. 5*G*), this interface is disrupted in the mutant form, indicating that the single point mutation by A-to-I editing could affect the physical interaction between SLC22A3 and ACTN4. These results suggest that wild-type SLC22A3 is directly associated with ACTN4 and inhibits ACTN4-mediated actin crosslinking.

We next tested whether wild-type SLC22A3 attenuated ACTN4-mediated cell invasion. RNAi was used to knock down endogenous ACTN4 expression in wild-type or edited KYSE30 cells overexpressing *SLC22A3*. Western blotting results showed that siRNA against ACTN4 could significantly reduce ACTN4 expression in wild-type or edited cells overexpressing *SLC22A3* and in empty-vector control cells (Fig. 6*A*). The cell invasion assay found that depletion of ACTN4 in edited cells overexpressing *SLC22A3* resulted in reduced invasiveness compared with control cells, whereas depletion of ACTN4 in wild-type cells overexpressing *SLC22A3* had no effects on cell invasion (Fig. 6*B*). Similarly, silencing endogenous ACTN4 expression in wild-type *SLC22A3*-repressed NE1 cells also showed decreased invasiveness compared with control cells (Fig. 6 *C* and *D*). ACTN4 induces cell motility by cross-linking actin filaments into bundles to form filopodia, activity controlled by the Rho family GTPase Cdc42 at the cellular periphery (32). Considering this effect, we assessed the expression of Cdc42 by Western blotting and filopodia formation by phalloidin staining in wild-type or edited KYSE30 clones overexpressing *SLC22A3* and *SLC22A3*-repressed NE1 clones 48 h after transfection of ACTN4

siRNA or control siRNA. We found that depletion of ACTN4 in edited KYSE30 cells overexpressing *SLC22A3* or *SLC22A3*-repressed NE1 cells displayed reduced Cdc42 expression (Fig. 6 *A* and *C*) and filopodia formation compared with control cells (Fig. 6*E*). All these data strongly suggest that wild-type *SLC22A3* may act as a metastasis suppressor by directly inhibiting ACTN4.

Collectively, we propose a disease model in which the deregulation of *SLC22A3*, predisposed in individuals at high risk of familial ESCC, could accelerate the cell motility of esophageal epithelial cells by reducing the inhibition of the actin-binding protein ACTN4, leading to the early malignant progression of ESCC (Fig. 6*F*).

Discussion

Cancer is a complex disease characterized by both genetic and epigenetic alterations. Here, we provide evidence that *SLC22A3* transcription is dramatically lower in NT esophageal epithelia from familial ESCCs than in those from sporadic ESCCs. A-to-I RNA editing at codon 72 (Asn→Asp) of *SLC22A3* may serve as an additional epigenetic mechanism relevant to esophageal cancer susceptibility. A link between A-to-I RNA editing and cancer has been established in the past few years (33–38). Until now, only a few proteins with amino acid substitutions that are caused by a single site-specific RNA-editing event have been reported with validity, and there is no apparent causal relationship between altered RNA-editing levels and the initiation of cancer progression. Our group reported that an A-to-I RNA–editing event at codon 367 (Ser→Gly) of antizyme inhibitor 1 (AZIN1)
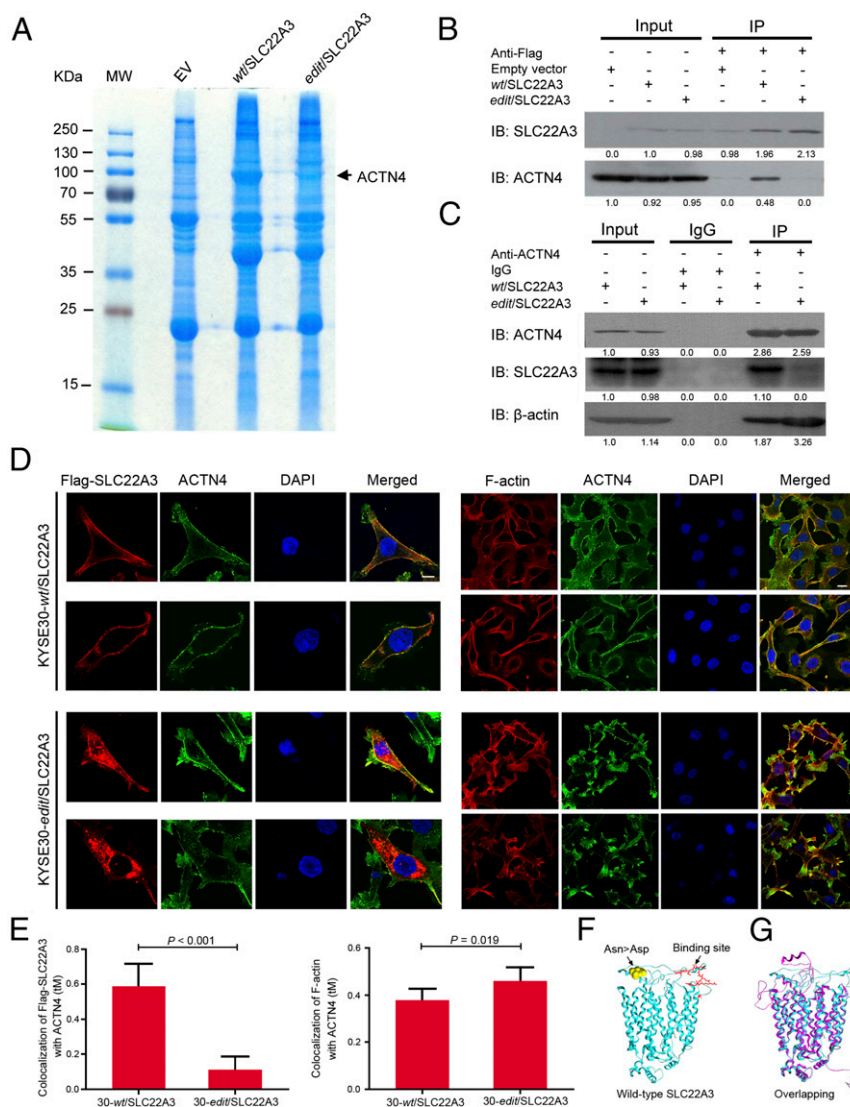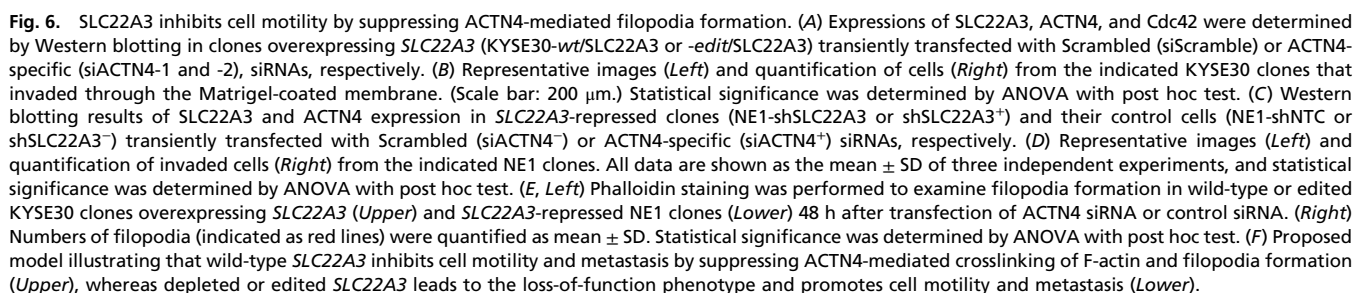
Fig. 5. SLC22A3 interacts with ACTN4 and inhibits ACTN4-mediated actin crosslinking. (*A*) Identification of SLC22A3-associated proteins from Flag-tagged wild-type or edited *SLC22A3* (*wt*/SLC22A3 or *edit*/SLC22A3) transfected KYSE30 cells by IP and mass spectrometry. The gel was stained with Coomassie blue. Parallel IP from empty-vector (EV)–transfected KYSE30 was performed as a negative control. (*B*) Whole-cell extracts from KYSE30-*wt*/SLC22A3 and -*edit*/SLC22A3 were immunoprecipitated with anti-Flag–conjugated beads. Immunoprecipitants were subjected to Western blotting for SLC22A3 or ACTN4. Parallel IP from empty-vector–transfected KYSE30 was performed as a negative control. (*C*) Whole-cell extracts from KYSE30-*wt*/SLC22A3 and -*edit*/SLC22A3 were immunoprecipitated with ACTN4 antibody, followed by immunoblotting for ACTN4 or SLC22A3, respectively. Mouse IgG was used as a negative control. (*D*) KYSE30-*wt*/SLC22A3 and -*edit*/SLC22A3 cells were double immunolabeled with anti-Flag (red)/anti-ACTN4 (green) (*Left*) and anti–F-actin (red)/anti-ACTN4 (green) (*Right*) antibodies, respectively. Nuclei were counterstained with DAPI (blue). (Magnification: 400×.) (Scale bars: 20 μm.) (*E*) Quantification of colocalization between Flag-SLC22A3 (*Left*) or F-actin (*Right*) and ACTN4 in KYSE30-*wt*/SLC22A3 and -*edit*/SLC22A3 cells, performed by ZEN 2012 software. Each column represents the mean ± SD for tM (the sum of the colocalized red pixels divided by the sum of the total red pixels), with ~50–100 cells analyzed per colocalization replicate. (*F*) Structural model of the wild-type form of protein SLC22A3 (cyan). The edited residue Asn > Asp is highlighted as yellow spheres, and a predicted protein interface with ACTN4 is shown as red sticks. (*G*) The wild-type (cyan) and the edited (purple) protein structures of SLC22A3 were superimposed to show their differences.

is a gain-of-function event and may be a potential driver in the pathogenesis of HCC (34). Intriguingly, our current study found that A-to-I *SLC22A3* RNA editing occurs almost exclusively in familial high-risk individuals but not in sporadic ESCC, indicating a strong genetic association between *SLC22A3* RNA editing and esophageal cancer susceptibility. *SLC22A3*-positive editing in familial NT tissues is also well correlated with a decreased level of *SLC22A3* mRNA. This observation is in line with previous reports that RNA editing may influence transcript stability, as characterized by altered transcription levels of the editing targets (39, 40).

Taking advantage of previously reported GWASs in ESCC (26, 27), we found *ADAR2* (or *ADARB1*), one of the three RNA editing

enzymes (ADAR1, ADAR2, and ADAR3) identified as catalyzing A-to-I RNA editing, to be a susceptibility gene on 21q22.3 for familial ESCC. In our study, *ADAR2* is overexpressed and positively correlated with *SLC22A3* editing in familial NT esophageal tissues. However, ADAR1 and ADAR3 are barely expressed in NT esophageal tissues as previously reported (41). These data suggested that aberrant expression of *ADAR2* may specifically change the coding sequence of *SLC22A3* in high-risk individuals with a family history of ESCC.

Functionally, we found that *SLC22A3* is a metastasis-suppressor gene in esophageal cancer. A metastasis-suppressor gene is defined as a gene in which loss of function specifically enhances metastasis without affecting primary tumor growth (42).

Fig. 6. SLC22A3 inhibits cell motility by suppressing ACTN4-mediated filopodia formation. (*A*) Expressions of SLC22A3, ACTN4, and Cdc42 were determined by Western blotting in clones overexpressing *SLC22A3* (KYSE30-*wt*/SLC22A3 or -*edit*/SLC22A3) transiently transfected with Scrambled (siScramble) or ACTN4-specific (siACTN4-1 and -2), siRNAs, respectively. (*B*) Representative images (*Left*) and quantification of cells (*Right*) from the indicated KYSE30 clones that invaded through the Matrigel-coated membrane. (Scale bar: 200 μm.) Statistical significance was determined by ANOVA with post hoc test. (*C*) Western blotting results of SLC22A3 and ACTN4 expression in *SLC22A3*-repressed clones (NE1-shSLC22A3 or shSLC22A3$^+$) and their control cells (NE1-shNTC or shSLC22A3$^-$) transiently transfected with Scrambled (siACTN4$^-$) or ACTN4-specific (siACTN4$^+$) siRNAs, respectively. (*D*) Representative images (*Left*) and quantification of invaded cells (*Right*) from the indicated NE1 clones. All data are shown as the mean ± SD of three independent experiments, and statistical significance was determined by ANOVA with post hoc test. (*E, Left*) Phalloidin staining was performed to examine filopodia formation in wild-type or edited KYSE30 clones overexpressing *SLC22A3* (*Upper*) and *SLC22A3*-repressed NE1 clones (*Lower*) 48 h after transfection of ACTN4 siRNA or control siRNA. (*Right*) Numbers of filopodia (indicated as red lines) were quantified as mean ± SD. Statistical significance was determined by ANOVA with post hoc test. (*F*) Proposed model illustrating that wild-type *SLC22A3* inhibits cell motility and metastasis by suppressing ACTN4-mediated crosslinking of F-actin and filopodia formation (*Upper*), whereas depleted or edited *SLC22A3* leads to the loss-of-function phenotype and promotes cell motility and metastasis (*Lower*).

A series of in vitro and in vivo assays showed that *SLC22A3* could suppress cell migration/invasion and EMT process in esophageal cancer cells and inhibit lymph node metastasis in severe combined immunodeficient (SCID) mice but has no influence on cell growth and clonogenicity. Separately from the studies in esophageal cancer cells, we also looked for a role of *SLC22A3* in normal esophageal epithelial cells. Reduced *SLC22A3* could promote cell motility in normal esophageal cells, strongly suggesting that *SLC22A3* may drive early cell migration and invasion in the pathogenesis of ESCC. Further study revealed that membrane localization of wild-type *SLC22A3* was able to inhibit cell motility by binding directly to ACTN4 and suppressing ACTN4-mediated actin crosslinking and filopodia formation. ACTN4 belongs to the α-actinin family of actin-binding and crosslinking proteins. Assembly of these cell structural proteins is believed to play a crucial role in stress fiber

formation, promoting cell adhesion and regulating cell shape and motility (43, 44). Emerging evidence shows that ACTN4 is implicated in cancer cell migration/invasion, metastasis, and the EMT process (28, 45–47). Intriguingly, our previous study also found that increased expression of ACTN4 is significantly correlated with lymph node metastasis and may serve as a stage-specific marker for esophageal cancer (48). In contrast, edited or reduced *SLC22A3* could accelerate cell motility by decreasing the capability to bind ACTN4. These findings revealed molecular basis underlying the early development and poor prognosis of familial ESCC.

In summary, our study demonstrates that A-to-I RNA editing renders a loss-of-function phenotype for the metastasis suppressor *SLC22A3* in individuals at high risk of familial esophageal cancer. Our study also illustrates one mechanism by which wild-type *SLC22A3* attenuates cell motility by binding directly to the

metastasis-promoting protein ACTN4; this observation may provide insights into the early development and progression of familial ESCC and lead to more effective management of high-risk individuals with *SLC22A3* deregulation.

Materials and Methods

Additional details about the experimental procedures, including descriptions of RNA/DNA extraction, qPCR, microarray analysis, PCR cloning, lentiviral transduction, in vitro functional assays, coimmunoprecipitation, mass spectrometry, immunofluorescence staining, and Western blotting, are provided in *SI Materials and Methods*.

Ethics Statement. The study was approved by the Institutional Review Board (IRB) of the University of Hong Kong. Written informed consents were obtained for the original human work that produced the tissue samples. Animal experiments were approved by the Committee on the Use of Live Animals in Teaching and Research (CLATR) of the University of Hong Kong.

Clinical Specimens. Specimens from familial and sporadic ESCC cohorts from the Linzhou People's Hospital and Anyang Cancer Hospital in Henan and the Sun Yat-Sen University Cancer Center in Guangzhou were collected between 2005 and 2013. Snap-frozen specimens of tumors and surrounding NT esophageal tissues were collected from patients with familial and sporadic ESCC at the Linzhou People's Hospital ($n = 104$ cases; including 54 familial and 50 sporadic cases), Anyang Cancer Hospital ($n = 72$ cases; 27 familial and 45 sporadic cases), and the Sun Yat-Sen University Cancer Center ($n = 50$ cases, all sporadic). A familial case was defined as a patient having at least one blood relative with ESCC within three generations, as detailed in Table S4.

Pyrosequencing Analyses. RT-PCR was first performed using the primers for pyrosequencing listed in Table S5. The reverse primer was labeled with biotin. The single-stranded biotinylated PCR products then were processed for pyrosequencing analysis, as described previously (34), using the sequencing primers listed in Table S5. The template-sequencing primer mixture was transferred into a PSQ 96 Plate (Biotage), heated to 90 °C for 2 min, and cooled to room temperature. Sequencing reactions were performed with a PSQ 96 SNP Reagent Kit (Biotage) using a PSQ 96MA instrument (Biotage) according to the manufacturer's instructions. Experiments were performed in triplicate. The sample genotype and percent heteroplasmy were determined using the allele frequency quantification (AQ) function in the SNP software (Biotage). The sensitivity of pyrosequencing is usually 5%. Therefore, we designate samples with a G signal >5% as positive editing in our study.

Post Hoc GWAS Study. Based on the dataset of a previously reported esophageal cancer GWAS (27), we conducted genotyping data analyses by selecting 291 SNPs in an ∼1.2-Mb region covering the *ADAR2* gene on 21q22 from 496 cases with a family history of upper gastrointestinal tract cancers and 1,056 healthy controls. We then examined potential genetic relatedness based on pairwise identity by state for all of the successfully genotyped samples using PLINK 1.07 software. The original script from EIGENSTRAT was modified to extract principal components for plotting, as described previously (49). The association results for selected 21q SNPs are summarized in Table S6.

In Vivo Lymph Node Metastasis Assay. The study protocol for the lymph node metastasis assay was approved by and performed in accordance with the Committee on the Use of Live Animals in Teaching and Research at The University of Hong Kong. Four- to six-week-old SCID mice were injected s.c. through the footpad with 2×10^5 cells in PBS. Animals were killed 45 d later. The popliteal lymph nodes were isolated and fixed in 10% formalin, followed by H&E staining.

Prediction of Protein Structure and Interface. Structural models of the wild-type and RNA-edited proteins were built with Rebetta [robetta.bakerlab.org/]. The main part of the model was based on a homolog structure, rat GLUT5 [Protein Data Bank (PDB) ID code 4YBQ, www.rcsb.org/] (50), and the rest of the fragments were constructed ab initio. Structural comparison was done using GRASP2 (30) to superimpose the wild-type and the edited proteins. The potential binding interfaces of the wild-type protein were predicted by using cons-PPISP (31).

Statistical Analysis. The statistical analyses were performed with SPSS standard version 16.0 (SPSS, Inc.). The *SLC22A3* expression levels in the tumors and their matched NT tissues or in groups stratified by editing status were compared using the Mann–Whitney U test. The independent Student's t test was used to compare the values of the colocalization threshold Manders' (tM) coefficients in wild-type and edited *SLC22A3* transfected cells. ANOVA with post hoc test was used to compare in vitro cell function and relative expression levels of the target genes between different groups. A χ^2 test was used to compare the frequencies of editing, clinicopathological features in patients, and numbers of mice with lymph node metastasis in the different groups. The correlation between the mRNA level of *SLC22A3*/*ADAR2* and the editing level of *SLC22A3* was analyzed using Spearman's correlation. A P value less than 0.05 was considered statistically significant.

1. Torre LA, et al. (2015) Global cancer statistics, 2012. *CA Cancer J Clin* 65:87–108.
2. Pickens A, Orringer MB (2003) Geographical distribution and racial disparity in esophageal cancer. *Ann Thorac Surg* 76:S1367–S1369.
3. Wheeler JB, Reed CE (2012) Epidemiology of esophageal cancer. *Surg Clin North Am* 92:1077–1087.
4. Thrift AP, et al.; Australian Cancer Study Clinical Follow-Up Study (2012) The influence of prediagnostic demographic and lifestyle factors on esophageal squamous cell carcinoma survival. *Int J Cancer* 131:E759–E768.
5. Zhao P, Dai M, Chen W, Li N (2010) Cancer trends in China. *Jpn J Clin Oncol* 40:281–285.
6. Castellsagué X, et al. (2000) Influence of mate drinking, hot beverages and diet on esophageal cancer risk in South America. *Int J Cancer* 88:658–664.
7. Ke L (2002) Mortality and incidence trends from esophagus cancer in selected geographic areas of China circa 1970-90. *Int J Cancer* 102:271–274.
8. Carter CL, et al. (1992) Segregation analysis of esophageal cancer in 221 high-risk Chinese families. *J Natl Cancer Inst* 84:771–776.
9. Hu N, et al. (1992) Familial aggregation of oesophageal cancer in Yangcheng County, Shanxi Province, China. *Int J Epidemiol* 21:877–882.
10. Hu N, et al. (2003) Evidence for a familial esophageal cancer susceptibility gene on chromosome 13. *Cancer Epidemiol Biomarkers Prev* 12:1112–1115.
11. Hu N, et al. (2005) Allelotyping of esophageal squamous-cell carcinoma on chromosome 13 defines deletions related to family history. *Genes Chromosomes Cancer* 44:271–278.
12. Huang J, et al. (2000) High frequency allelic loss on chromosome 17p13.3-p11.1 in esophageal squamous cell carcinomas from a high incidence area in northern China. *Carcinogenesis* 21:2019–2026.
13. Su H, et al. (2003) Gene expression analysis of esophageal squamous cell carcinoma reveals consistent molecular profiles related to a family history of upper gastrointestinal cancer. *Cancer Res* 63:3872–3876.
14. Hu N, et al. (2009) Genomic characterization of esophageal squamous cell carcinoma from a high-risk population in China. *Cancer Res* 69:5908–5917.
15. Wen D, et al. (2009) Early onset, multiple primary malignancies, and poor prognosis are indicative of an inherited predisposition to esophageal squamous cell carcinoma for the familial as opposed to the sporadic cases–an update on over 14-year survival. *Eur J Med Genet* 52:381–385.
16. Lu P, et al. (2014) Genome-wide gene expression profile analyses identify CTTN as a potential prognostic marker in esophageal cancer. *PLoS One* 9:e88918.
17. Eeles RA, et al.; UK Genetic Prostate Cancer Study Collaborators; British Association of Urological Surgeons' Section of Oncology; UK ProtecT Study Collaborators (2008) Multiple newly identified loci associated with prostate cancer susceptibility. *Nat Genet* 40:316–321.
18. Cui R, et al. (2011) Common variant in 6q26-q27 is associated with distal colon cancer in an Asian population. *Gut* 60:799–805.
19. Grisanzio C, et al. (2012) Genetic and functional analyses implicate the NUDT11, HNF1B, and SLC22A3 genes in prostate cancer pathogenesis. *Proc Natl Acad Sci USA* 109:11252–11257.
20. Wu X, et al. (1998) Identity of the organic cation transporter OCT3 as the extra-neuronal monoamine transporter (uptake2) and evidence for the expression of the transporter in the brain. *J Biol Chem* 273:32776–32786.
21. Koepsell H (2004) Polyspecific organic cation transporters: Their functions and interactions with drugs. *Trends Pharmacol Sci* 25:375–381.
22. Chen L, et al. (2013) Genetic and epigenetic regulation of the organic cation transporter 3, SLC22A3. *Pharmacogenomics J* 13:110–120.

23. Huang W, Sherman BT, Lempicki RA (2009) Systematic and integrative analysis of large gene lists using DAVID bioinformatics resources. *Nat Protoc* 4:44–57.
24. Skobe M, et al. (2001) Induction of tumor lymphangiogenesis by VEGF-C promotes breast cancer metastasis. *Nat Med* 7:192–198.
25. Nishikura K (2010) Functions and regulation of RNA editing by ADAR deaminases. *Annu Rev Biochem* 79:321–349.
26. Wu C, et al. (2011) Genome-wide association study identifies three new susceptibility loci for esophageal squamous-cell carcinoma in Chinese populations. *Nat Genet* 43:679–684.
27. Wang LD, et al. (2010) Genome-wide association study of esophageal squamous cell carcinoma in Chinese subjects identifies susceptibility loci at PLCE1 and C20orf54. *Nat Genet* 42:759–763.
28. Barbolina MV, et al. (2008) Motility-related actinin alpha-4 is associated with advanced and metastatic ovarian carcinoma. *Lab Invest* 88:602–614.
29. Weins A, et al. (2007) Disease-associated mutant alpha-actinin-4 reveals a mechanism for regulating its F-actin-binding affinity. *Proc Natl Acad Sci USA* 104:16080–16085.
30. Petrey D, Honig B (2003) GRASP2: Visualization, surface properties, and electrostatics of macromolecular structures and sequences. *Methods Enzymol* 374:492–509.
31. Chen H, Zhou HX (2005) Prediction of interface residues in protein-protein complexes by a consensus neural network method: Test against NMR data. *Proteins* 61:21–35.
32. Nobes CD, Hall A (1995) Rho, rac, and cdc42 GTPases regulate the assembly of multimolecular focal complexes associated with actin stress fibers, lamellipodia, and filopodia. *Cell* 81:53–62.
33. Paz N, et al. (2007) Altered adenosine-to-inosine RNA editing in human cancer. *Genome Res* 17:1586–1595.
34. Chen L, et al. (2013) Recoding RNA editing of AZIN1 predisposes to hepatocellular carcinoma. *Nat Med* 19:209–216.
35. Han SW, et al. (2014) RNA editing in RHOQ promotes invasion potential in colorectal cancer. *J Exp Med* 211:613–621.
36. Han L, et al. (2015) The genomic landscape and clinical relevance of A-to-I RNA editing in human cancers. *Cancer Cell* 28:515–528.
37. Paz-Yaacov N, et al. (2015) Elevated RNA editing activity is a major contributor to transcriptomic diversity in tumors. *Cell Reports* 13:267–276.
38. Nakano M, Fukami T, Gotoh S, Nakajima M (2017) A-to-I RNA editing up-regulates human dihydrofolate reductase in breast cancer. *J Biol Chem* 292:4873–4884.
39. Kim DD, et al. (2004) Widespread RNA editing of embedded alu elements in the human transcriptome. *Genome Res* 14:1719–1725.
40. Dominissini D, Moshitch-Moshkovitz S, Amariglio N, Rechavi G (2011) Adenosine-to-inosine RNA editing meets cancer. *Carcinogenesis* 32:1569–1577.
41. Qin YR, et al. (2014) Adenosine-to-inosine RNA editing mediated by ADARs in esophageal squamous cell carcinoma. *Cancer Res* 74:840–851.
42. Nguyen DX, Massagué J (2007) Genetic determinants of cancer metastasis. *Nat Rev Genet* 8:341–352.
43. Honda K, et al. (1998) Actinin-4, a novel actin-bundling protein associated with cell motility and cancer invasion. *J Cell Biol* 140:1383–1393.
44. Shao H, Wang JH, Pollak MR, Wells A (2010) α-actinin-4 is essential for maintaining the spreading, motility and contractility of fibroblasts. *PLoS One* 5:e13921.
45. Honda K, et al. (2005) Actinin-4 increases cell motility and promotes lymph node metastasis of colorectal cancer. *Gastroenterology* 128:51–62.
46. Kikuchi S, et al. (2008) Expression and gene amplification of actinin-4 in invasive ductal carcinoma of the pancreas. *Clin Cancer Res* 14:5348–5356.
47. An HT, Yoo S, Ko J (2016) α-Actinin-4 induces the epithelial-to-mesenchymal transition and tumorigenesis via regulation of Snail expression and β-catenin stabilization in cervical cancer. *Oncogene* 35:5893–5904.
48. Fu L, et al. (2007) Identification of alpha-actinin 4 and 67 kDa laminin receptor as stage-specific markers in esophageal cancer by proteomic approaches. *Cancer* 110:2672–2681.
49. Deng M, et al. (2013) Genome-wide association analyses in Han Chinese identify two new susceptibility loci for amyotrophic lateral sclerosis. *Nat Genet* 45:697–700.
50. Berman HM, et al. (2000) The Protein Data Bank. *Nucleic Acids Res* 28:235–242.
51. Shimada Y, Imamura M, Wagata T, Yamaguchi N, Tobe T (1992) Characterization of 21 newly established esophageal cancer cell lines. *Cancer* 69:277–284.
52. Zhang C, et al. (2009) Fibroblast growth factor receptor 2-positive fibroblasts provide a suitable microenvironment for tumor development and progression in esophageal carcinoma. *Clin Cancer Res* 15:4017–4027.